The cristal membrane of mitochondria is the principal site of oxidative phosphorylation

Robert W. Gilkerson, Jeanne M.L. Selker, Roderick A. Capaldi*

Institute of Molecular Biology, University of Oregon, Eugene, OR 97403-1229, USA

Received 18 February 2003; revised 20 April 2003; accepted 23 May 2003

First published online 11 June 2003

Edited by Vladimir Skulachev

Abstract The inner membrane system of mitochondria is known to consist of two contiguous but distinct membranes: the inner boundary membrane, which apposes the outer membrane, and the cristal membrane, which forms tubules or lamellae in the interior. Using immunolabeling and transmission electron microscopy of bovine heart tissue, we have calculated that around 94% of both Complex III of the respiratory chain and the ATP synthase are located in the cristal membrane, and only around 6% of either is in the inner boundary membrane. When accounting for the topographical ratio of cristal membrane versus inner boundary membrane, we find that both complexes exist at a 2.2–2.6-fold higher concentration in the cristal membrane. The residual protein in the inner boundary membrane may be newly assembled complexes destined for cristal membranes. Our results argue for restricted diffusion of complexes through the cristal junctions and indicate that the mitochondrial cristae comprise a regulated submitochondrial compartment specialized for ATP production.

Key words: Mitochondrion; Oxidative phosphorylation; Crista; Electron microscopy; Immunolabeling

1. Introduction

The mitochondrion is a membrane-bound organelle which performs a wide range of necessary functions, including ATP production, fatty acid oxidation, and participation in apoptosis, calcium homeostasis, and signaling by reactive oxygen species. Genomic and proteomic approaches are currently being used to catalog the thousands of proteins located within the mitochondrion [1,2]. In addition, the structure and dynamics of the mitochondrial network are being evaluated in relation to the diverse functions of this organelle [3,4]. Structurally, mitochondria are composed of a number of compartments. The outer membrane bounds the organelle, while the inner membrane separates the extremely protein-dense matrix space from the intermembrane space [5]. The inner membrane system is composed largely of double-membrane interdigitations called cristae. These cristae were widely assumed to be loose infoldings of the inner membrane, but recent electron tomographic studies [6–10] have revealed that they are structurally distinct, in agreement with the model of mitochondrial structure first proposed by Sjostrand [11]. Thus, the inner membrane system is now best described as two contiguous but distinct membranes: the inner boundary membrane, which apposes the outer membrane, and the cristal membranes, which extend into the mitochondrial interior as tubules or lamellae. The cristal and inner boundary membranes are joined by a limited number of discrete sites called crista junctions, which typically have a consistent diameter of ~30 nm but may be altered by matrix volume and respiratory activity [7–10]. An obvious issue raised by the new structural data is whether the inner boundary and cristal membranes are compositionally and functionally distinct.

Traditionally, subfractionation of isolated mitochondria is used to localize proteins within the organelle (e.g. [12]), but such methods to date have not clearly separated inner boundary from cristal membranes. Therefore, we have examined the distribution of two complexes of oxidative phosphorylation (OXPHOS), Complex III – or ubiquinone cytochrome *c* oxidoreductase – and the ATP synthase, in situ by immunogold labeling of ultrathin sections of bovine heart tissue. Our results show that both complexes are located predominantly in cristal membranes.

2. Materials and methods

2.1. Spurr's fixation/embedment

Bovine heart tissue was obtained immediately postmortem and minced. Tissue was fixed for 4 h in 2.5% glutaraldehyde/4% paraformaldehyde in 0.1 M sodium cacodylate pH 7.4 with 8 mM $CaCl_2$, followed by postfixation in 1% OsO_4 in buffer. Samples were then sequentially dehydrated in ethanol and infiltrated with Spurr's resin. Blocks were polymerized by incubation at 60°C.

2.2. LR Gold immunolabeling

Bovine heart tissue was obtained immediately postmortem and minced. Tissue was then fixed for 4 h at room temperature in 0.4% glutaraldehyde/4% paraformaldehyde/3.5% sucrose in 0.1 M sodium phosphate buffer, pH 7.4, followed by postfixation in 2% uranyl acetate in 3.5% sucrose in 0.06 M maleate buffer on ice for 1 h. Tissue was then sequentially dehydrated in acetone and infiltrated with LR Gold acrylic resin (London Resin Company) after Berryman and Rodewald [13]. Ultrathin (60–75 nm) sections on 400 mesh nickel grids were equilibrated in Tris-buffered saline (TBS), pH 7.4, and then blocked for 20 min in 10% normal goat serum. Sections were incubated in monoclonal antibody solution by droplet flotation at 50 μg/ml in TBS 7.4. After washing five times through buffer, sections were incubated in 1:20 diluted secondary anti-mouse gold conjugate (Amersham) for 30 min. Sections were again washed five times through TBS 7.4 and then stabilized in 2% glutaraldehyde for 3 min.

*Corresponding author. Fax: (1)-541-346 4854.
E-mail address: rcapaldi@oregon.uoregon.edu (R.A. Capaldi).

Abbreviations: TBS, Tris-buffered saline; OXPHOS, oxidative phosphorylation

0014-5793/03/$22.00
doi:10.1016/S0014-5793(03)00633-1

Sections were washed five times through double-distilled H_2O. Sections were counterstained for 3 min in 2% OsO_4, followed by 3 min in lead citrate and carbon-stabilized.

2.3. Immunolabeling of ultrathin cryosections

Immunolabeling of cryosections was performed as per Murray et al. [14]. Briefly, tissue was fixed immediately postmortem in 0.1% glutaraldehyde/4% paraformaldehyde in 0.1 M sodium phosphate buffer. Tissue was washed, placed in 5% gelatin, and infiltrated overnight with 2.3 M sucrose in buffer at 4°C. Tissue was placed on sectioning pins and plunge-frozen in liquid nitrogen. Ultrathin (80–100 nm) cryosections were cut on a Reichert-Jung Ultracut microtome with an F4E cryochamber. Sections were blocked in 2% bovine serum albumin for 10 min and incubated in primary monoclonal antibody at 55–60 μg/ml. Secondary antibody incubations were performed as for LR Gold-embedded material. Sections were contrasted in 0.4% uranyl acetate in 2% methyl cellulose for 5 min and dried. Ultrathin cryosections were viewed at 80 kV.

2.4. Microscopy and image analysis

Sections were viewed on a Philips CM12 transmission electron microscope at 60 kV except where noted. Negatives were scanned in Adobe Photoshop and subsequent image analysis performed in NIH Image.

3. Results

To characterize the structure of mitochondria in bovine heart tissue, we first examined tissue embedded in Spurr's resin. Spurr's resin is not amenable to immunolabeling of protein complexes, but it offers excellent membrane contrast due to the use of osmium tetroxide during the embedding process, so that morphometric analysis is optimized. When viewed by transmission electron microscopy, bovine heart tissue is dominated by longitudinal arrays of myofibrils composed of actin–myosin filaments with many mitochondria arranged alongside to provide ATP. The mitochondria have many cristae of a consistent diameter (26 ± 3 nm), indicative of tubular, rather than lamellar, cristae (Fig. 1). The appearance of circular cristal profiles in transverse sections is consistent with predominantly tubular cristal organization (data not shown). These cristae join the inner boundary membrane at discrete crista junctions of 27 ± 4 nm (Fig. 1, inset). The cristal width is consistently larger than the outer+inner boundary membrane width (26 vs. 17 nm), indicating that the intracristal space is larger than the intermembrane space. When cristal and inner boundary membranes were traced using NIH Image, these membranes were found to exist at a ratio of 6.2:1, respectively (Table 1). A second set of experiments was conducted with cryosectioned heart tissue, conditions facilitating good immunolabeling of proteins. No significant differences were observed in morphology and the ratio of cristal to boundary membrane was again 6.2:1. Therefore, the method of fixation did not determine the observed mitochondrial structure. Our findings for the dimensions of the novel structural features are in good agreement with measurements using neuronal and brown adipose tissues [6,7,15].

Both LR Gold sections and cryosections were immunolabeled for Complex III and the F_1F_0 ATP synthase (Fig. 2A). Immunolabeled LR Gold sections displayed heavy labeling throughout the interior of the mitochondria for both complexes. By contrast, a monoclonal antibody against porin, an outer membrane-localized protein [16], gave labeling only at the periphery of the mitochondrial profile, as expected based on the known outer membrane localization of this protein (Fig. 2B). No appreciable extramitochondrial labeling was detected. Negative controls, using both non-specific normal mouse immunoglobulin (Fig. 2D) and omission of primary antibody (not shown) showed extremely low background levels. Two different sizes of secondary gold were used: 10 nm, because of the ease of detection, and 5 nm, because of better penetration into the sections. As expected, there was more labeling with the smaller probe, but both gave the same ratio of labeling in the two membranes.

Immunolabeling of ultrathin cryosections yielded similar results. Note that cryosections display reversed contrast

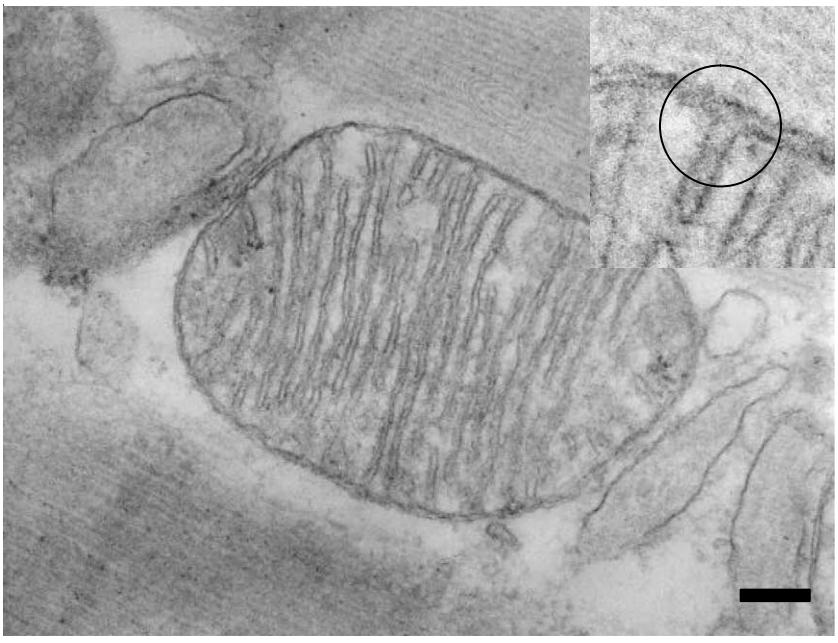

Fig. 1. Bovine heart mitochondrial structure. Electron micrograph of Spurr's embedded bovine heart tissue showing mitochondrial structure. Cristae are clearly apparent as numerous membrane compartments traversing the mitochondrial interior. Cristae join the inner boundary membrane at discrete crista junctions, diverting away from the inner boundary membrane at right angles (inset, circled). Size bar 0.25 μ.

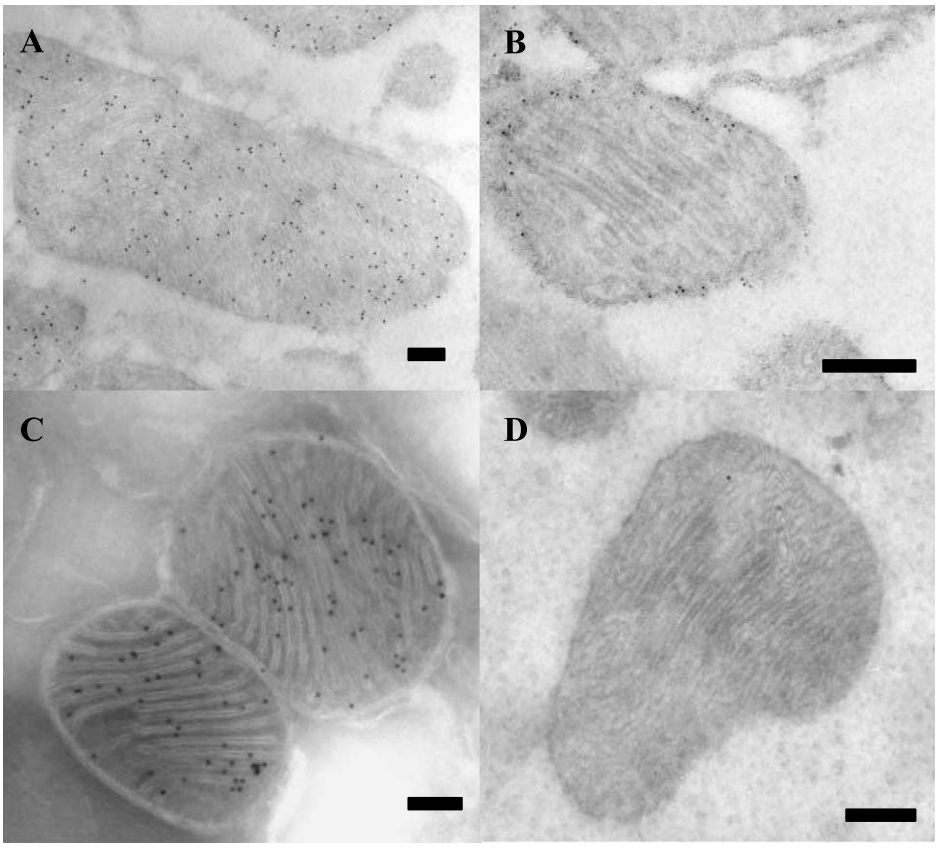

Fig. 2. Immunolabeling of mitochondria in bovine heart tissue. Immunolabeled ultrathin sections of bovine heart tissue, showing distribution of mitochondrial proteins. A: LR Gold ultrathin section labeled with anti-$F_1\alpha$ primary (ATP synthase), 10 nm gold-conjugated secondary antibody. B: LR Gold ultrathin section labeled with anti-porin primary, 5 nm secondary antibody. C: Ultrathin cryosection labeled with anti-Core 2 primary (Complex III), 10 nm secondary antibody. D: LR Gold negative control section, normal mouse IgG primary, 10 nm secondary antibody. Size bars 0.25 μ.

Table 1
Distribution of OXPHOS proteins between the cristal and inner boundary membranes

	Labeling density[a]	Total particles			
		CM[b]	IBM[c]	CM/IBM	[CM]/[IBM][d]
Membrane trace				6.2[e]	1 ± 0.23, $n = 6$
LR Gold:					
Complex III					
10 nm	93.4	1730	121	14.3	2.31 ± 0.55, $n = 14$
5 nm	159	1074	77	14.0	2.26 ± 0.56, $n = 10$
ATP synthase					
10 nm	81.3	1088	76	14.3	2.31 ± 0.92, $n = 10$
5 nm	243	1302	82	15.8	2.55 ± 0.75, $n = 12$
Normal mouse IgG					
10 nm	3				
5 nm	4				
No primary					
10 nm	0.5				
5 nm	4				
Cryosections:					
Complex III					
10 nm	101	1146	72	15.9	2.57 ± 0.53, $n = 16$
ATP synthase					
10 nm	49	427	29	14.7	2.37, $n = 10$

[a]Antibody labeling signal in counts/μ^2.
[b]CM = cristal membrane.
[c]IBM = inner boundary membrane.
[d]CM/IBM divided by 6.2 (ratio of cristal to inner boundary membrane).
[e]A morphometric model of the cristal membrane as a tubule reveals the CM/IBM membrane ratio to be ~3:1, suggesting an even greater cristal enrichment of OXPHOS proteins than expressed; however, in the absence of tomographic data the cristal membrane is rendered linearly.

when compared with LR Gold sections, with membranes appearing as light outlines against a dark field (Fig. 2C).

A quantitative analysis of the labeling of the inner boundary and cristal membranes by antibodies to the two complexes is given in Table 1. For this analysis, the location of each gold particle was sorted initially into three classes: (i) ones definitively in cristal membranes and more than 15 nm from the inner boundary membrane; (ii) ones in the inner boundary membrane and 15 nm away from a cristal junction; and (iii) those within 15 nm of a clearly identified cristal membrane. Because of the size of the primary plus secondary antibodies, class iii particles are ambiguously located and, for the final analysis, we divided them equally into class i or class ii. For both Complex III and the ATP synthase, the ratio of the distribution between cristal membranes and inner boundary membranes was between 14:1 and 16:1, irrespective of the embedding method or the size of the gold particle. Taking account of the different areas of the two membranes, the density of Complex III and the ATP synthase in the cristal membrane is ~2.5 times that in the inner boundary membrane.

4. Discussion

Our data show that around 94% of Complex III and the ATP synthase respectively are in cristal membranes and only around 6% of these OXPHOS complexes are located in the inner boundary membrane, corresponding to a 2.2–2.6-fold enrichment of these complexes within the cristal membrane when the topographical ratio of cristal and inner boundary membrane is factored in. This finding leads to two important conclusions. It is the most definitive evidence so far that the cristal membrane is the principal site of OXPHOS. Previous studies have examined the distribution of another OXPHOS component, cytochrome *c* oxidase in mitochondria, by histochemistry, taking advantage of the oxidation of diaminobenzidine by the enzyme, but these have led to conflicting results [7,17,18]. There are other, more indirect, observations to support the idea that the cristal membrane is specialized for OXPHOS. Rho^0 cells, lacking mitochondrial DNA, and hence unable to use OXPHOS for ATP synthesis, have very little cristal membrane but a normal inner boundary membrane [19]. Among the functions of the inner boundary membrane is the transport of ions and substrates to maintain cellular homeostasis, along with protein import at sites that involve contacts between it and the outer membrane [20]. Assembly of the respiratory chain and ATP synthase requires both proteins imported from the cytosol, and mitochondrially synthesized subunits. Assembly of these complexes likely takes place at the inner boundary membrane, thereby accounting for the small amount of OXPHOS components detected in this membrane. Additionally, the inner boundary membrane is likely dominated by transporters such as the adenine nucleotide translocase, leaving no space for such an enrichment of OXPHOS complexes as we observe in the cristal membrane.

An important implication of the present work is that diffusion of complexes between the cristal and inner boundary membrane may be restricted, once the cristae are formed. This implies that the crista junction is a barrier to diffusion between the two membranes, consistent with the suggestion of Frey et al. [7] that the crista junction is a thermodynamically favorable arrangement of the mitochondrial inner membrane which may mediate compartmentation of OXPHOS complexes.

Acknowledgements: R.W.G. was supported by National Institutes of Health Training Grant GM07759. We thank James Murray for insight and comments on the manuscript. We also thank Devin Oglesbee for assistance with manuscript preparation.

References

[1] Taylor, S.W., Fahy, E., Zhang, B., Glenn, G.M., Warnock, D.E., Wiley, S., Murphy, A.N., Gaucher, S.P., Capaldi, R.A., Gibson, B.W. and Ghosh, S.S. (2003) Nat. Biotechnol. 21, 281–286.
[2] Fountoulakis, M., Berndt, P., Langen, H. and Suter, L. (2002) Electrophoresis 23, 311–328.
[3] Collins, T.J., Berridge, M.J., Lipp, P. and Bootman, M.L. (2002) EMBO J. 21, 1616–1627.
[4] Margineantu, D., Cox, W., Sundell, L., Sherwood, S., Beechem, J. and Capaldi, R.A. (2002) Mitochondrion 1, 397–478.
[5] Saraste, M. (1999) Science 283, 1488–1493.
[6] Perkins, G., Renken, C., Martone, M.E., Young, S.J., Ellisman, M. and Frey, T.J. (1997) J. Struct. Biol. 119, 260–272.
[7] Frey, T.G., Renken, C.W. and Perkins, G.A. (2002) Biochim. Biophys. Acta 1555, 196–203.
[8] Frey, T.G. and Mannella, C.A. (2000) Trends Biochem. Sci. 25, 319–324.
[9] Mannella, C.A., Marko, M. and Buttle, K. (1997) Trends Biochem. Sci. 22, 37–38.
[10] Mannella, C.A., Marko, M., Penczek, P., Barnard, D. and Frank, J. (1994) Microsc. Res. Tech. 27, 278–283.
[11] Sjostrand, F.S. (1953) Nature (Lond.) 171, 30–32.
[12] Satoh, M., Hamamoto, T., Seo, N., Kagawa, Y. and Endo, H. (2003) Biochem. Biophys. Res. Commun. 300, 482–493.
[13] Berryman, M.A. and Rodewald, R.D. (1990) J. Histochem. Cytochem. 38, 159–170.
[14] Murray, J.G., Gilkerson, R.W. and Capaldi, R.A. (2002) FEBS Lett. 529, 173–178.
[15] Perkins, G.A., Song, J.Y., Tarsa, L., Deerinck, T.J., Ellisman, M.H. and Frey, T.G. (1998) J. Bioenerg. Biomembr. 30, 431–442.
[16] Yu, W.H., Wolfgang, W. and Forte, M. (1995) J. Biol. Chem. 270, 13998–14006.
[17] Hiraoka, T. and Hirai, K.I. (1992) J. Electron. Microsc. 41, 127–129.
[18] Perotti, M.E., Anderson, W.A. and Swift, H. (1983) J. Histochem. Cytochem. 31, 351–365.
[19] Gilkerson, R.W., Margineantu, D.H., Capaldi, R.A. and Selker, J.M.L. (2000) FEBS Lett. 474, 1–4.
[20] Hoogenraad, N.J. and Ryan, M.T. (2001) IUBMB Life 51, 345–350.